Letter

Fundamental distinction between intrinsic and extrinsic nonlinear thermal Hall effects

Da-Kun Zhou [1], Zhi-Fan Zhang [1], Xiao-Qin Yu [2,*], Zhen-Gang Zhu [1,3,4,†] and Gang Su [1,4,5,‡]

[1] *Theoretical Condensed Matter Physics and Computational Materials Physics Laboratory, College of Physical Sciences, University of Chinese Academy of Sciences, Beijing 100049, China*

[2] *School of Physics and Electronics, Hunan University, Changsha 410082, China*

[3] *School of Electronic, Electrical and Communication Engineering, University of Chinese Academy of Sciences, Beijing 100049, China*

[4] *CAS Center for Excellence in Topological Quantum Computation, University of Chinese Academy of Sciences, Beijing 100190, China*

[5] *Kavli Institute of Theoretical Sciences, University of Chinese Academy of Sciences, Beijing 100049, China*

(Received 8 October 2021; revised 14 March 2022; accepted 19 April 2022; published 4 May 2022)

We theoretically investigated the fundamental distinction between the intrinsic and extrinsic nonlinear thermal Hall effects in the presence of disorder at the second-order response to the temperature gradient in terms of the semiclassical Boltzmann equation. We found that, at low temperatures, the intrinsic contribution of the nonlinear thermal Hall conductivity is proportional to the square of temperature, whereas the extrinsic contributions (side jump and skew scattering) are independent of temperature. This distinct dependency on temperature provides an approach to readily distinguish between the intrinsic and extrinsic contributions. Specifically, we analyzed the nonlinear thermal Hall effect for a tilted two-dimensional massive Dirac material. In particular, we showed that when the Fermi energy is located at the Dirac point, the signal is solely from the intrinsic mechanism; when the Fermi energy is higher, the extrinsic contributions are dominant, which are two to three orders of magnitude larger than the intrinsic contribution.

DOI: 10.1103/PhysRevB.105.L201103

Introduction. Traditionally, Hall (Nernst) effects are studied in linear-response regimes, namely, the generated transverse voltage is linearly proportional to the driving forces (electric field or temperature gradient). Broken time-reversal symmetry due to the presence of magnetization or an external magnetic field is required to guarantee such a Hall voltage. Recently, a nonlinear anomalous Hall effect [1–10] (NAHE) as a second-harmonic response to an ac electric field has been proposed and attracted broad interests in the study of nonlinear anomalous transport phenomena in time-reversal invariant but inversion symmetry broken materials. The most interesting fact is that this NAHE is owing to the emergent Berry curvature dipole in the momentum space rather than the Berry curvature itself. It reveals the complicated interplay between the nontrivial topological structure of the energy bands and the transverse Hall-like transport [1–6]. NAHE was predicted in several noncentrosymmetric materials, such as bilayer WTe_2 [2], strained graphene [3], and the topological crystalline insulator SnTe [11], etc., and has been successfully observed in bilayer [12] and few-layer [13] WTe_2. In addition, it was found that NAHE has broad applications due to its characteristics [14–19], for example, it can be used to make strain sensors [14] and rectifiers [15].

Although the origin of the anomalous Hall effect was thought to be from an intrinsic [20] (disorder-free) or extrinsic (disorder-induced) contribution that includes side jumps [21] and skew scattering [22], it is still a challenge to identify these contributions experimentally. So far, there are two main approaches, namely the traditional [20–30] and the new scaling law [31–33], to distinguish between different mechanisms. In the conventional scaling law, the skew-scattering contribution to the anomalous Hall effect can be easily distinguished from the intrinsic and side-jump contributions through the scaling relations between the induced Hall resistance and the longitudinal resistivity ρ_{xx}, namely $\rho_{\rm int} \propto \rho_{xx}^2$ [20], $\rho_{\rm sj} \propto \rho_{xx}^2$ [21], $\rho_{\rm sk} \propto \rho_{xx}$ [22]. However, the contribution from the intrinsic mechanism or side jump cannot be further identified. Unlike the traditional scaling law in which the scaling $\rho_{\rm AH} = f(\rho_{xx})$ depends only on the single-scattering-induced ρ_{xx}, the new scaling $\rho_{\rm AH} = f(\rho_i, \rho_{xx})$ (where $\rho_{xx} = \sum_i \rho_i$) considers the involved multiple competing scatterings and also depends on the partial longitudinal resistivity ρ_i stemming from the involved scattering sources [31–33], such as phonons or impurities. In experiments, the partial resistivity generated by different scattering sources needs first be determined, and then one needs to determine the contribution of each mechanism through fitting scaling parameters. Recently, Lu *et al.* applied the basic idea of the new scaling law to the nonlinear-response regime [8] to distinguish between the intrinsic and extrinsic contributions to the nonlinear anomalous Hall effect.

The thermal Hall effect refers to a generation of transverse heat current as a response to a longitudinal temperature gradient, which can be carried not only by electrons [34–36], but also by magnons [37,38], phonons [39–41], and photons [42]. Recently, the thermal Hall effect has been extended to the nonlinear regime and an intrinsic nonlinear thermal Hall effect originated from the Berry curvature was reported in

*yuxiaoqin@hnu.edu.cn
†zgzhu@ucas.ac.cn
‡gsu@ucas.ac.cn

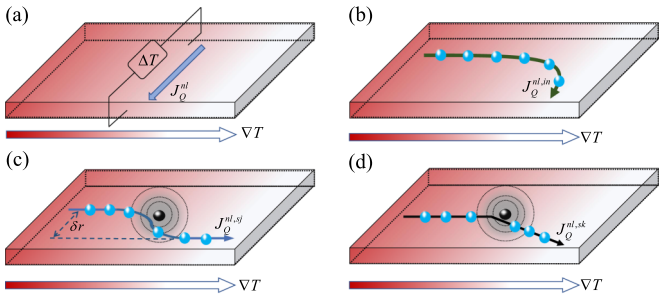

FIG. 1. (a) Schematic illustration of the nonlinear thermal Hall effect (NTHE) as a second-order response to the temperature gradient where the nonlinear thermal Hall current (NTHC) is $\mathbf{j}^{\rm nl} \propto (\boldsymbol{\nabla} T)^2$. The generation of NTHE stems from (b) an intrinsic contribution, (c) side jumps, and (d) skew scattering. The black ball in (c) and (d) represents disorder.

clean systems with time-reversal symmetry [43], in which a transverse heat current is generated vertically to the temperature gradient and scales quadratically with the temperature gradient. Usually, defects and impurities are inevitable in authentic materials. In this Letter, we investigate an electron-carried nonlinear thermal Hall effect (NTHE) in the presence of disorder by taking into account both intrinsic and extrinsic contributions in time-reversal invariant and noncentrosymmetric materials (Fig. 1). We focus that the temperature dependence of the induced nonlinear thermal Hall conductivity (NTHC) κ_{yxx} is $\kappa_{yxx}^{\rm in} \propto T^2$, $\kappa_{yxx}^{\rm sj} \propto T^0$, $\kappa_{yxx}^{\rm sk} \propto T^0$ at low temperatures, which also provides another approach to distinguish between the intrinsic contribution ($\propto T^2$) from the extrinsic contribution ($\propto T^0$) that can be easily tested experimentally.

General theory. Within the framework of semiclassical theory, the total thermal Hall currents in the absence of electric field as a response to the temperature gradient in the presence of a nontrivial Berry curvature $\Omega(\mathbf{k})$ and disorder [see details in the Supplemental Material (SM) [44]] is found to be

$$\mathbf{j}_Q^T = \sum_n \int [d\mathbf{k}][E_n(\mathbf{k}) - \mu] f_l \left(\mathbf{v} + \mathbf{v}_l^{\rm sj}\right) + \frac{\boldsymbol{\nabla} T}{T} \times \frac{1}{\hbar} \sum_n \int [d\mathbf{k}][E_n(\mathbf{k}) - \mu] \boldsymbol{\Omega}_{\mathbf{n}}(\mathbf{k}) \times \{[E_n(\mathbf{k}) - \mu] f_l + k_{\rm B} T \log(1 + e^{-\beta[E_n(\mathbf{k}) - \mu]})\}, \quad (1)$$

where $l = (n, \mathbf{k})$ is a combined index with the energy band n and momentum $\mathbf{k}$, $E_n(\mathbf{k})$ denotes the energy dispersion, $\mathbf{v}$ represents the group velocity, μ indicates the chemical potential (Fermi energy), $\mathbf{v}_l^{\rm sj} = \sum_{l'} \varpi_{ll'} \delta \mathbf{r}_{l'l}$ is the side-jump velocity originating from a disorder-induced coordinate shift $\delta \mathbf{r}_{l'l}$ [45], and the nonequilibrium distribution function f_l can be expressed as $f_l = f_l^{\rm in} + \delta f_l^{\rm sk}$ in the presence of a temperature gradient and disorder, where $\delta f_l^{\rm sk}$ is the skew-scattering-induced modification. The total heat current $\mathbf{j}_Q^T$ in Eq. (1) thus can be decomposed into four parts as $\mathbf{j}_Q^T = \mathbf{j}_Q^{\rm N} + \mathbf{j}_Q^{\rm in} + \mathbf{j}_Q^{\rm sj} + \mathbf{j}_Q^{\rm sk}$ corresponding to the conventional, intrinsic, side-jump, and skew-scattering contributions to the heat current, respectively [44]. It has been shown that the standard conventional heat current $\mathbf{j}_Q^{\rm N}$ comes from the conventional velocity in time-reversal invariant materials [44].

The linear thermal Hall current as a first-order response to the temperature gradient will disappear in time-reversal invariant materials. That is because the linear thermal conductivity is a symmetric tensor by Onsager's reciprocity relations in the presence of time-reversal symmetry [46]. The linear heat current is aligned to the direction of the temperature gradient, leading to the vanishing of linear thermal Hall current. Therefore, only the nonlinear heat current possibly flows vertically to the temperature gradient in the presence of time-reversal symmetry. Through solving the Boltzmann equation, the nonequilibrium distribution function f_l to the second-order correction to the temperature gradient can be determined [44]. Accompanying the formulas of $\mathbf{j}_Q^{\rm in}$, $\mathbf{j}_Q^{\rm sj}$, and $\mathbf{j}_Q^{\rm sk}$ in the SM [44], the nonlinear thermal Hall current $\mathbf{j}^{\rm nl}$ (where the superscript "nl" refers to nonlinear) in the a direction, as the response to the second order in the temperature gradient, is found to be [44]

$$j_a^{\rm nl} \equiv -\kappa_{abd} \partial_b T \partial_d T, \quad (2)$$

where κ_{abd} is a coefficient characterizing the nonlinear thermal Hall effect and its formulas from three mechanisms are given in the SM [44]. Analogous to the nonlinear anomalous Hall effect [1] and the nonlinear anomalous Nernst effect [47] induced by the Berry curvature dipole, it is found that only the states near the Fermi surface make contributions to the intrinsic NTHE, which is in contrast to the extrinsic contribution. Through the Sommerfeld expansion [44], the coefficients k_{abb} due to the intrinsic, side-jump, and skew-scattering mechanisms at low temperature are found, respectively, to be

$$\kappa_{abb}^{\rm in} = -\frac{7\tau\pi^4 k_B^4}{15\hbar^2} T^2 G_0'(\mu) + O[(k_B T)^4], \quad (3)$$

$$\kappa_{abb}^{\rm sj} = -\frac{1}{3}\tau^2 \pi^2 k_B^2 F_0(\mu) + O[(k_B T)^2], \quad (4)$$

$$\kappa_{abb}^{\rm sk} = \frac{\tau^3 \pi^2 k_B^2}{3\hbar} g_0(\mu) + O[(k_B T)^2]. \quad (5)$$

where $G_0(\mu)$, $F_0(\mu)$, and $g_0(\mu)$ (given in the SM [44]) are Fermi-energy-dependent parameters and independent of temperature. According to Eqs. (3)–(5), one finds that the leading order of NTHC from these three contributions has the following temperature T dependence: $\kappa_{abb}^{\rm in} \propto T^2$, $\kappa_{abb}^{\rm sj} \propto T^0$, $\kappa_{abb}^{\rm in} \propto T^0$. Through this temperature dependence, the intrinsic contribution ($\propto T^2$) can be easily distinguished from the extrinsic contribution ($\propto T^0$), which provides another approach to identify the intrinsic and extrinsic mechanisms in experiments. This scheme is different from the previous scaling law in which the dependence of anomalous Hall resistivity on the longitudinal resistivity is applied to distinguish between the intrinsic and extrinsic contributions. We found that the use of temperature dependence in NTHE to distinguish between intrinsic and extrinsic mechanisms is exclusive. We investigate three mechanisms in the linear and nonlinear order of the anomalous Hall effect, anomalous Nernst effect, and anomalous thermal Hall effect, respectively, and

showed that only in NTHE can we distinguish between intrinsic and extrinsic mechanisms using temperature dependence [44].

Model. By exploiting the symmetry analysis, the nonvanishing NTHC can exist in time-reversal invariant and inversion symmetry broken materials. We note that the NTHC tensor has the same symmetry dependence as the nonlinear anomalous Hall conductivity (NAHC) tensor. Specifically, this consistency is reflected in the intrinsic (or side-jump, or skew-scattering) contribution of the NTHC tensor and the NAHC tensor has the same matrix form under the same point group [10]. The noncentrosymmetric monolayer transition-metal dichalcogenides (TMDCs) is one of the candidates to observe the nonlinear thermal Hall effect, and the low-energy structure of TMDCs can be described by a simple tilted two-dimensional (2D) massive Dirac model [8], namely

$$\hat{\mathcal{H}}_0 = tk_x + v(k_x\sigma_x + k_y\sigma_y) + m\sigma_z, \tag{6}$$

where $\sigma_{x,y,z}$ are the Pauli matrices, and t, v, and m are related model parameters. t is a band tilting parameter which tilts the Dirac cone along the x direction, and $2m$ is the gap. As the time reversal of the model contributes equally to the nonlinear thermal Hall current, it is sufficient to study this model only. This Hamiltonian considers only one Dirac cone. Indeed, there is another inequivalent Dirac cone (the time-reversal counterpart of this model) which, however, contributes equally to the nonlinear thermal Hall current. $\hat{\mathcal{H}}_0$ is invariant under the mirror operation M_x about the x-y plane. The energy eigenvalue is $E_n(\mathbf{k}) = tk_x + nE_0(\mathbf{k})$ with $E_0(\mathbf{k}) = \sqrt{v^2k^2 + m^2}$ where $n = \pm 1$ in $E_n(\mathbf{k})$ represents the band index. The Berry curvature is $\Omega^n_{\mathbf{k}} = -n\frac{mv^2}{2(E_0(\mathbf{k}))^3}$. In fact, in the x-y plane, the Berry curvature is a pseudovector, and only the z component Ω^n_z exists.

In order to investigate the extrinsic contribution to the NTHE induced by disorder, we consider a δ-function random potential $\hat{V}_{\text{imp}}(\mathbf{r}) = \sum_i V_i\delta(\mathbf{r} - \mathbf{R}_i)$ with $\mathbf{R}_i$ indicating the random position of impurities and V_i representing the disorder strength, which satisfies $\langle V_i\rangle_{\text{dis}} = 0$, $\langle V_i^2\rangle_{\text{dis}} = V_0^2 \neq 0$, and $\langle V_i^3\rangle_{\text{dis}} = V_1^3 \neq 0$ [48]. To analyze the behavior of NTHE of the tilted 2D massive Dirac model, we consider the $t \ll v$ limit and treat the relaxation time τ momentum independent, namely $\frac{1}{\tau} = \frac{n_iV_0^2}{4\hbar}\frac{\mu^2+3m^2}{v^2\mu}$ [8], where n_i represents the impurity concentration.

After a careful derivation (see details in the SM [44]), we found $\kappa^{\text{in/sk/sj}}_{xyy} = 0$ and $\kappa^{\text{in/sk/sj}}_{yxx} \neq 0$. This suggests that only when applying the temperature gradient in the x direction perpendicular to the mirror line M_x (the subscript x means that the mirror plane is perpendicular to the x direction), there is a nonzero nonlinear thermal Hall current due to both the intrinsic and extrinsic mechanisms in the y direction (perpendicular to the temperature gradient and parallel to the M_x). In other words, once applying the temperature gradient in the y direction, the nonlinear thermal Hall current will disappear as required by the mirror symmetry M_x. The nonzero κ_{yxx} to the first order of the band tilting strength t in the intrinsic, side-jump, and skew-scattering mechanisms for the tilted 2D massive Dirac model in the presence of disorder at low temperature are derived analytically,

$$\kappa^{\text{in}}_{yxx} = \frac{7\pi^3tmk_B^2}{5\hbar n_iV_0^2}\frac{v^2(\mu^2-2m^2)}{\mu^4(\mu^2+3m^2)}(k_BT)^2,$$
$$\kappa^{\text{sj}}_{yxx} = -\frac{\pi tmk_B^2}{6\hbar n_iV_0^2}\frac{v^2(\mu^2-m^2)(5\mu^2-9m^2)}{\mu^2(\mu^2+3m^2)}, \tag{7}$$

and

$$\kappa^{\text{sk}}_{yxx} = \frac{\pi v^2tmk_B^2}{3\hbar n_i^2V_0^6/V_1^3}\frac{(\mu^2-m^2)(\mu^2-2m^2)}{\mu(\mu^2+3m^2)^3} + \frac{\pi v^2tmk_B^2}{2\hbar n_iV_0^2}\frac{(\mu^2-m^2)(3\mu^2-5m^2)}{\mu^2(\mu^2+3m^2)^3}, \tag{8}$$

respectively. According to Eqs. (7) and (8), at low temperature, the nonlinear thermal Hall coefficient from the intrinsic and extrinsic mechanisms can be identified through the temperature dependence of $\kappa^{\text{tot}}_{yxx}$ since the intrinsic κ^{in}_{yxx} displays a quadratic dependence on temperature whereas both κ^{sj}_{yxx} and κ^{sk}_{yxx} are independent of temperature. The total $\kappa^{\text{tot}}_{yxx}$ can be written as $\kappa^{\text{tot}}_{yxx} = \alpha T^2 + \lambda$ where the coefficients α and λ represent the contribution from intrinsic and extrinsic mechanisms, respectively, and can be measured in future experiments.

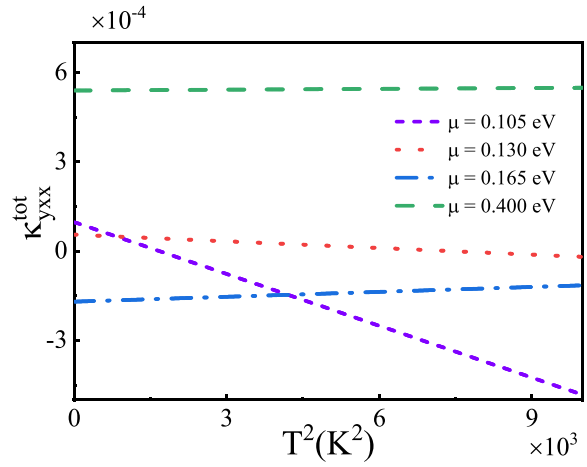

FIG. 2. Total nonlinear thermal Hall conductivity $\kappa^{\text{tot}}_{xxy}$ vs temperature at different Fermi energies. Here, the unit for the y axes is k_B^2 Å/$\hbar$. Parameters are taken as $t = 0.1$ eV Å, $v = 1$ eV Å, $m = 0.1$ eV, $n_iV_0^2 = 10^2$ eV^2 Å^2, and $n_iV_1^3 = 10^4$ eV^3 Å^4.

Figure 2 displays the total NTHC $\kappa^{\text{tot}}_{yxx}$ as a function of T^2 at different Fermi energies for the titled 2D massive Dirac model. The intercept (λ) and the slope multiplied by the square of temperature (αT^2) give the magnitudes of the extrinsic-mechanism-induced $\kappa^{\text{ex}}_{yxx} = \kappa^{\text{sj}}_{yxx} + \kappa^{\text{sk}}_{yxx}$ and intrinsic-mechanism-induced κ^{in}_{yxx}, respectively. The enhanced intercept and decreased slope at a higher Fermi energy indicate that the extrinsic contribution is gradually dominant. The signal of κ_{yxx} from the extrinsic contribution is almost 245 times larger than that from the intrinsic contribution when the Fermi energy is taken at 0.4 eV and the temperature is fixed at 50 K. However, when the Fermi energy is near the bottom of the conduction band (e.g., $\mu = 0.105$ eV), the slope becomes sharper and the intrinsic contribution is strengthened. It is observed that the

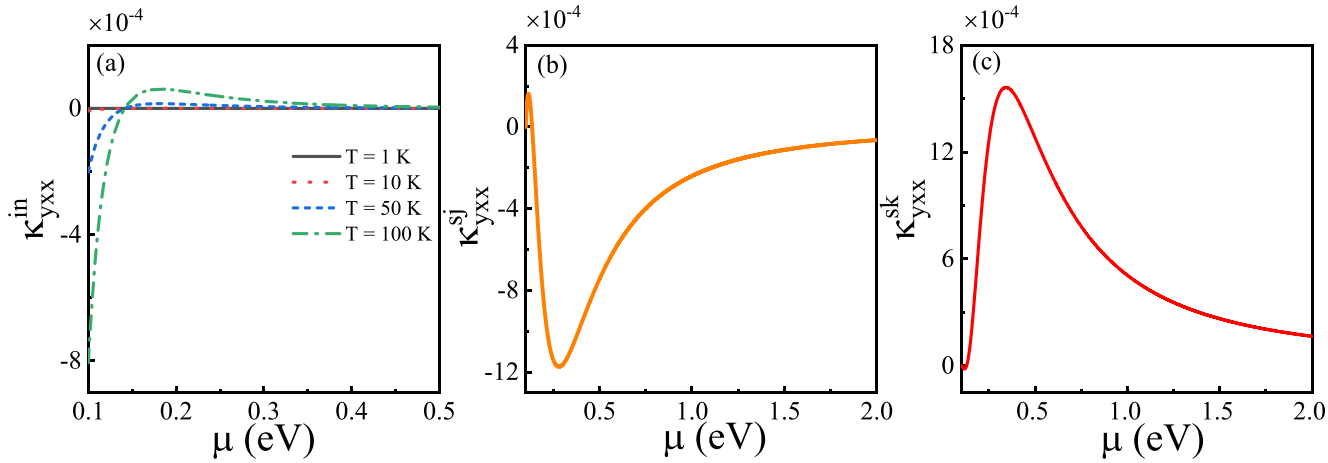

FIG. 3. (a) Intrinsic, (b) side-jump, and (c) skew-scattering contributions to the nonlinear thermal Hall conductivity κ_{yxx} in a tilted 2D massive Dirac model vs Fermi energy at different temperatures, respectively. Here, the unit for the y axes is k_B^2 Å$/\hbar$, and the other parameters are the same as in Fig. 2.

magnitude of αT^2 at 50 K is equal to 1.49λ for $\mu = 0.105$ eV, implying that both contributions from intrinsic and extrinsic mechanisms to NTHE become comparable.

In addition to the temperature dependence, the Fermi energy dependence of the NTHC can be used to identify these three scattering mechanisms (see Fig. 3). For $\mu = 0.1$ eV, the Fermi level is just entering into the bottom of the conduction band, $\kappa^{\rm sj}_{yxx}$ and $\kappa^{\rm sk}_{yxx}$ tend to zero, and only $\kappa^{\rm in}_{yxx}$ is finite [Figs. 3(a)–3(c)], revealing that all the heat current flowing vertically to the temperature gradient at the Dirac point would stem solely from the intrinsic contribution. This band-edge case may be a supplemental identification to the T-dependence identification. Since the Fermi level can be tuned in the TMDCs by a gate voltage, it is instructive to study the Fermi energy dependence further. $\kappa^{\rm in}_{yxx}$ drops dramatically with increasing $\mu > 0.1$ eV and changes its sign from negative to positive (about $\mu = 0.14$ eV). It grows into a peak and finally decays to zero at large μ. $\kappa^{\rm sj}_{yxx}$ is almost negative when the Fermi level enters into the conduction band, and it develops a dip around $\mu = 0.28$ eV and finally tends to zero. The variation of $\kappa^{\rm sk}_{yxx}$ on the Fermi energy is similar to that of $\kappa^{\rm sj}_{yxx}$ but with an opposite sign. The peak of $\kappa^{\rm sk}_{yxx}$ is around $\mu = 0.34$ eV. Combining all three components of κ_{yxx}, the total $\kappa^{\rm tot}_{yxx}$ starts at a negative value ($\mu = 0.1$ eV, intrinsic component), drops dramatically with increasing μ and changes into a positive one, develops into a positive peak, and finally decays to zero at large μ. It is seen that the positive $\kappa^{\rm tot}_{yxx}$ is basically coming from side-jump and skew-scattering contributions but the skew scattering dominates.

We should emphasize here that our calculation has a limitation on the temperature range. The present model corresponds to some two-dimensional materials in which the Fermi level is actually aligned into a band. Thus, these materials in fact behave as metals rather than insulators. Therefore, heat transfer is expected to be mediated basically by the conduction electrons or holes rather than phonons [49]. The temperature limit of our calculation is mainly limited by the method used, i.e., the Sommerfeld expansion, leading us to Eqs. (3)–(5). It shows that for temperatures lower than 90 K, the second-order expansion gives a correction of less than 5%.

Conclusions. In summary, we studied the nonlinear thermal Hall effect in the presence of disorder as a second-order response of the temperature gradient. Remarkably, it is revealed that, at low temperature, the intrinsic-mechanism-induced nonlinear thermal Hall conductivity is proportional to the square of temperature, while the extrinsic-mechanism-induced nonlinear thermal Hall conductivity is independent of temperature, which presents another approach to clarify the intrinsic and extrinsic contributions. We also analyzed the nonlinear thermal Hall effect for a tilted 2D Dirac material with mirror symmetry M_x. It is found that the mirror symmetry M_x has a strong limitation on the nonlinear thermal Hall conductivity: Only when the temperature gradient is applied perpendicular to the mirror line, a finite nonlinear thermal Hall current can be generated. Moreover, it is shown that as the Fermi energy enters into the bottom of the conduction band, the signal is solely from the intrinsic mechanism. At high Fermi levels, the signal from the extrinsic mechanism (mainly skew scattering) will dominate.

Acknowledgments.. This work is supported by NSFC (Grants No. 11974348, No. 11674317, and No. 11834014) and the Fundamental Research Funds for the Central Universities. G.S. and Z.G.Z. are supported in part by the National Key R&D Program of China (Grant No. 2018FYA0305800), the Strategic Priority Research Program of CAS (Grants No. XDB28000000 and No. XDB33000000). X.Q.Y. is supported by NSFC (Grant No. 12004107) and the Fundamental Research Funds for the Central Universities.

[1] I. Sodemann and L. Fu, Phys. Rev. Lett. **115**, 216806 (2015).

[2] Z. Z. Du, C. M. Wang, H.-Z. Lu, and X. C. Xie, Phys. Rev. Lett. **121**, 266601 (2018).

[3] R. Battilomo, N. Scopigno, and G. Oxtix, Phys. Rev. Lett. **123**, 196403 (2019).

[4] T. Low, Y. Jiang, and F. Guinea, Phys. Rev. B **92**, 235447 (2015).

[5] J. I. Facio, D. Efremov, K. Koepernik, J.-S. You, I. Sodemann, and J. van den Brink, Phys. Rev. Lett. **121**, 246403 (2018).

[6] J.-S. You, S. Fang, S.-Y. Xu, E. Kaxiras, and T. Low, Phys. Rev. B **98**, 121109(R) (2018).

[7] S. Nandy and I. Sodemann, Phys. Rev. B **100**, 195117 (2019).

[8] Z. Z. Du, C. M. Wang, S. Li, H.-Z. Lu, and X. C. Xie, Nat. Commun. **10**, 3047 (2019).

[9] Z. Z. Du, H.-Z. Lu, and X. C. Xie, Nat. Rev. Phys. **3**, 744 (2021); T. Ideue and Y. Iwasa, Annu. Rev. Condens. Matter Phys. **12**, 201 (2021).

[10] Z. Z. Du, C. M. Wang, H.-P. Sun, H.-Z. Lu, and X. C. Xie, Nat. Commun. **12**, 5038 (2021).

[11] A. Lau and C. Ortix, Phys. Rev. Lett. **122**, 186801 (2019).

[12] Q. Ma, S.-Y. Xu, H. Shen, D. MacNeill, V. Fatemi, T.-R. Chang, A. M. M. Valdivia, S. Wu, Z. Du, C.-H. Hsu, S. Fang, Q. D. Gibson, K. Watanabe, T. Taniguchi, R. J. Cava, E. Kaxiras, H.-Z. Lu, H. Lin, L. Fu, N. Gedik *et al.*, Nature (London) **565**, 337 (2018).

[13] K. Kang, T. Li, E. Sohn, J. Shan, and K. F. Mak, Nat. Mater. **18**, 324 (2019).

[14] R. C. Xiao, D. F. Shao, Z. Q. Zhang, and H. Jiang, Phys. Rev. Applied **13**, 044014 (2020)

[15] H. Isobe, S. Y. Xu, and L. Fu, Sci. Adv. **6**, eaay2497 (2020).

[16] Y. Zhang and L. Fu, Proc. Natl. Acad. Sci. USA **118**, e2100736118 (2021).

[17] J. Xiao, Y. Wang, H. Wang, C. D. Pemmaraju, S. Wang, P. Muscher, E. J. Sie, C. M. Nyby, T. P. Devereaux, X. Qian, X. Zhang, and A. M. Lindenberg, Nat. Phys. **16**, 1 (2020).

[18] P. Bhalla, A. H. MacDonald, and D. Culcer, Phys. Rev. Lett. **124**, 087402 (2020).

[19] K. W. Kim, T. Morimoto, and N. Nagaosa, Phys. Rev. B **95**, 035134 (2017).

[20] R. Karplus, and J. M. Luttinger, Phys. Rev. **95**, 1154 (1954).

[21] L. Berger, Phys. Rev. B **2**, 4559 (1970).

[22] J. Smit, Physica **24**, 39 (1958).

[23] W. Jellinghaus and M. P. de Andrés, Ann. Phys. (Leipzig) **462**, 189 (1961).

[24] P. N. Dheer, Phys. Rev. **156**, 637 (1967).

[25] W. L. Lee, S. Watauchi, V. L. Miller, R. J. Cava, and N. P. Ong, Science **303**, 1647 (2004).

[26] Y. Pu, D. Chiba, F. Matsukura, H. Ohno, and J. Shi, Phys. Rev. Lett. **101**, 117208 (2008).

[27] A. Fert and O. Jaoul, Phys. Rev. Lett. **28**, 303 (1972).

[28] C. Zeng, Y. Yao, Q. Niu, and H. H. Weitering, Phys. Rev. Lett. **96**, 037204 (2006).

[29] J. Kötzler and W. Gil, Phys. Rev. B **72**, 060412(R) (2005).

[30] J. Lavine, Phys. Rev. **123**, 1273 (1961).

[31] Y. Tian, L. Ye, and X. F. Jin, Phys. Rev. Lett. **103**, 087206 (2009).

[32] D. Hou, G. Su, Y. Tian, X. Jin, S. A. Yang, and Q. Niu, Phys. Rev. Lett. **114**, 217203 (2015).

[33] D. Yue and X. F. Jin, J. Phys. Soc. Jpn. **86**, 011006 (2017).

[34] Y. Shiomi, Y. Onose, and Y. Tokura, Phys. Rev. B **79**, 100404(R) (2009).

[35] W. Long, H. Zhang, and Q. F. Sun, Phys. Rev. B **84**, 075416 (2011).

[36] N. M. R. Peres, J. M. B. Lopes dos Santos, and T. Stauber, Phys. Rev. B **76**, 073412 (2007).

[37] Y. Onose, T. Ideue, H. Katsura, Y. Shiomi, N. Nagaosa, and Y. Tokura, Science **329**, 297 (2010).

[38] S. Murakami, and A. Okamoto, J. Phys. Soc. Jpn. **86**, 011010 (2017).

[39] T. Saito, K. Misaki, H. Ishizuka, and N. Nagaosa, Phys. Rev. Lett. **123**, 255901 (2019).

[40] C. Strohm, G. L. J. A. Rikken, and P. Wyder, Phys. Rev. Lett. **95**, 155901 (2005).

[41] T. Qin, J. Zhou, and J. Shi, Phys. Rev. B **86**, 104305 (2012).

[42] C. R. Otey, W. T. Lau, and S. Fan, Phys. Rev. Lett. **104**, 154301 (2010).

[43] C.-C. Zeng, S. Nandy, and S. Tewari, Phys. Rev. Research **2**, 032066(R) (2020).

[44] See Supplemental Material at http://link.aps.org/supplemental/10.1103/PhysRevB.105.L201103 for the derivation of equations in the main text.

[45] N. A. Sinitsyn, Q. Niu, and A. H. MacDonald, Phys. Rev. B **73**, 075318 (2006).

[46] L. D. Landau, E. M. Lifshitz, and L. P. Pitaevskii, in *Statistical Physics*, Course of Theoretical Physics Vol. 5, 3rd ed. (Pergamon Press, Oxford, UK, 1999).

[47] X.-Q. Yu, Z.-G. Zhu, J.-S. You, T. Low, and G. Su, Phys. Rev. B **99**, 201410(R) (2019).

[48] N. A. Sinitsyn, A. H. MacDonald, T. Jungwirth, V. K. Dugaev, and J. Sinova, Phys. Rev. B **75**, 045315 (2007).

[49] In metals, the speed of electrons (Fermi velocity) is much larger than that of phonons (speed of sound), and so is the specific heat. This makes the conduction electrons predominant in the thermal conduction in metals with weak disorder. Please see L. D. Landau and E. M. Lifshitz, *Physical Kinetics*, Course of Theoretical Physics (Pergamon Press, Oxford, UK, 1981), Vol. 10, Chap. IX.